CDK5 activator protein p25 preferentially binds and activates GSK3β

Hei-Man Chow[a], Dong Guo[b], Jie-Chao Zhou[b], Guan-Yun Zhang[b], Hui-Fang Li[b], Karl Herrup[a,c,1], and Jie Zhang[b,1]

[a]Division of Life Science and the State Key Laboratory of Molecular Neuroscience, Hong Kong University of Science and Technology, Kowloon, Hong Kong; [b]Fujian Provincial Key Laboratory of Neurodegenerative Disease and Aging Research, Institute of Neuroscience, College of Medicine, Xiamen University, Xiamen, Fujian 361102, People's Republic of China; and [c]Department of Cell Biology and Neuroscience, Rutgers University, Piscataway, NJ 08854

Edited by Thomas C. Südhof, Stanford University School of Medicine, Stanford, CA, and approved September 23, 2014 (received for review February 12, 2014)

Glycogen synthase kinase 3β (GSK3β) and cyclin-dependent kinase 5 (CDK5) are tau kinases and have been proposed to contribute to the pathogenesis of Alzheimer's disease. The 3D structures of these kinases are remarkably similar, which led us to hypothesize that both might be capable of binding cyclin proteins—the activating cofactors of all CDKs. CDK5 is normally activated by the cyclin-like proteins p35 and p39. By contrast, we show that GSK3β does not bind to p35 but unexpectedly binds to p25, the calpain cleavage product of p35. Indeed, overexpressed GSK3β outcompetes CDK5 for p25, whereas CDK5 is the preferred p35 partner. FRET analysis reveals nanometer apposition of GSK3β:p25 in cell soma as well as in synaptic regions. Interaction with p25 also alters GSK3β substrate specificity. The GSK3β:p25 interaction leads to enhanced phosphorylation of tau, but decreased phosphorylation of β-catenin. A partial explanation for this situation comes from in silico modeling, which predicts that the docking site for p25 on GSK3β is the AXIN-binding domain; because of this, p25 inhibits the formation of the GSK3β/AXIN/APC destruction complex, thus preventing GSK3β from binding to and phosphorylating β-catenin. Coexpression of GSK3β and p25 in cultured neurons results in a neurodegeneration phenotype that exceeds that observed with CDK5 and p25. When p25 is transfected alone, the resulting neuronal damage is blocked more effectively with a specific siRNA against *Gsk3β* than with one against *Cdk5*. We propose that the effects of p25, although normally attributed to activate CDK5, may be mediated in part by elevated GSK3β activity.

GSK3β | p25 | tau | β-catenin | neurodegeneration

Alzheimer's disease (AD) is the most common type of late-life dementia. Beginning predominantly after the age of 65, AD prevalence increases continuously with age (1). Pathologically, AD is characterized by cognitive impairment (2), progressive neurodegeneration (3), and the formation of amyloid-β (Aβ)-containing plaques and neurofibrillary tangles composed of hyperphosphorylated tau (4). During early stages of AD, the neurodegenerative process is characterized by synaptic damage accompanied by the loss of processes in the neocortex and limbic system (5). Indeed, synaptic loss remains as one of the strongest correlates to the cognitive decline in AD (6). At the level of mechanism, the aberrant activities of a number of signaling proteins, including cyclin-dependent kinase-5 (CDK5) (7) and glycogen synthase kinase-3β (GSK3β) (8), are also involved in the neurodegenerative progression of AD.

CDK5 is a widely expressed protein. As a proline-directed serine/threonine kinase, CDK5 is known to phosphorylate a number of cytoskeletal proteins (e.g., MAP1b, tau, neurofilament, nestin, DCX, CRMP2), synaptic proteins (e.g., PSD95, synapsin-I, E-cadherin), and transcription factors (MEF2) in postmitotic neurons (9, 10); its two activator proteins are p35 and p39. p35 and p39 resemble cyclins in their 3D structures and are almost exclusively detected in the nervous system; this restricts CDK5 activity largely to brain (11). CDK5 plays a pivotal role in neuronal development where its activity is required for normal neuronal migration and differentiation (12). CDK5 also contributes to neuronal health and survival after the developmental period has ended. Cdk5-deficient neurons are more vulnerable than wild-type cells to Aβ toxicity in culture (12, 13), more sensitive to DNA-damaging agents (14), and more susceptible to excitotoxic death (15). Our team has also recently reported that cytoplasmic CDK5 can attenuate Aβ-activated cell death (16).

Though clearly a positive influence on neurons in many different situations, the full picture of CDK5 action is more complicated because dysregulated CDK5 activity is also believed to contribute to neuronal death. When internal calcium concentrations rise, the calcium-dependent protease calpain is activated, resulting in the cleavage of p35 into p25. Although the levels of p25 are generally low in tissues, interaction with p25 has been reported to promote CDK5 stability and enhance its kinase activity (17), resulting in the abnormal phosphorylation of substrates such as tau (18). These data and others have led to the suggestion that CDK5 is potentially dysregulated in AD and that CDK5 inhibitors might have potential value as AD therapeutics (19).

GSK3 is another proline-directed serine/threonine kinase, originally identified as a key enzyme in regulating glycogen metabolism (20). GSK3 expression is ubiquitous, but its highest levels are found in the CNS, where it is recognized as a key regulator of neurogenesis (21), cellular polarization (22), neurite growth (23), and synaptic plasticity (24). In transgenic mouse models, constitutive GSK3 expression is found to be critical for neuronal viability (25). GSK3 activity is regulated at different levels. Phosphorylation of Tyr279/216 on GSK3α/β is important for enzymatic activity (26), whereas inactivation can be achieved through phosphorylation of Ser21/Ser9 residues. GSK3β is regulated in part by the WNT signaling pathway. In the absence of WNT, GSK3β interacts with AXIN and adenomatous polyposis coli (APC) to form a multiprotein complex (the destruction complex) that binds to and phosphorylates β-catenin (27).

Significance

CDK5 and GSK3β are recognized as interrelated kinases; they share a strong structural resemblance, and both are known tau kinases that contribute to the etiology of Alzheimer's disease. We report here that p25 but not p35, the normal cyclin-like activator of CDK5, unexpectedly binds to GSK3β in the AXIN-binding region. The binding of p25 increases GSK3β activity and alters its substrate specificity. Results, both in vivo and in vitro, suggest that many of the effects of p25 previously assumed to be due to hyperactivation of CDK5 must now be reexamined for the potential role of altered GSK3β activity. This result carries important implications for how we approach disease-modifying strategies for the treatment of Alzheimer's and other neurodegenerative diseases.

Author contributions: H.-M.C., D.G., K.H., and J.Z. designed research; H.-M.C., D.G., J.-C.Z., G.-Y.Z., H.-F.L., and J.Z. performed research; H.-F.L. contributed new reagents/analytic tools; H.-M.C., D.G., J.-C.Z., K.H., and J.Z. analyzed data; and H.-M.C., K.H., and J.Z. wrote the paper.

The authors declare no conflict of interest.

This article is a PNAS Direct Submission.

[1]To whom correspondence may be addressed. Email: jiezhang@xmu.edu.cn or herrup@ust.hk.

This article contains supporting information online at www.pnas.org/lookup/suppl/doi:10.1073/pnas.1402627111/-/DCSupplemental.

Despite these important roles in CNS development and maintenance, dysregulation of GSK3β activity, like that of CDK5, has been implicated in the progression AD; one obvious reason is that GSK3β is also known as tau protein kinase-1, and elevated levels of GSK3β activity are found in postmortem AD brains (28).

So far the effect of p25 on CDK5 function has been studied in vitro and in vivo, but remains poorly understood (17). It also has been previously reported that there is functional interaction between CDK5 and GSK3β (29). Based on the structural similarities between CDK5 and GSK3β, and previous data showing that CDK5 interacts with cyclins as well as with p35 and p39 (30), we asked whether these same regulator proteins were able to interact with and alter the activity or substrate specificity of GSK3β. Here we report that p25, but not p35 or other cyclins, binds directly to the residues within the T-loop and AXIN-binding channel in the C terminus of GSK3β. We find that p25 prefers binding to GSK3β over CDK5 when the three proteins are overexpressed together. Binding of p25 aberrantly activates the GSK3β kinase and alters its substrate specificity. The resulting aberrant activity severely reduces both neuritic arborization and synaptic density in cultures of cortical neurons. Targeted silencing of *Gsk3β* with siRNA protects neurons from these destructive effects more effectively than that specific for *Cdk5*. Our data show that p25 is a GSK3β regulator, and that this activity may contribute to the process of neurodegeneration.

Results

GSK3β Specifically Interacts with p25 But No Other Cyclins in Multiple Subcellular Locations. According to the human kinome, GSK3β and CDK5 belong to the CMGC kinase family (31), and share similar structural elements and arrangements with other CDKs, including the PSTAIRE/helix αC and an activation T-loop (32) (Fig. S1). We therefore speculated that GSK3β might also interact with activators of CDK5 or cyclins. We coexpressed HA-tagged GSK3β with green fluorescent protein-tagged p35 (GFP-p35), GFP-p25, or GFP-p10 in mouse N2a neuroblastoma cells. Coimmunoprecipitation (co-IP) with antibodies against HA (GSK3β) followed by Western blots of the immunoprecipitate with GFP showed that only p25, but not p35 or p10, can complex with GSK3β (Fig. 1*A*). This interaction appears to be specific for the CDK5 activator p25; neither cyclin A nor cyclin D1 showed evidence of meaningful binding to GSK3β (Fig. 1*B*). The failure to observe GSK3β interaction with cyclin A is significant because this cyclin has been noted to be similar to p25 in 3D structure (33).

To explore whether the GSK3β:p25 interaction was direct or indirect, we turned to FRET, which can only be achieved if the two fluorophores are located within a few nanometers of each other (34). We generated a set of GFP-tagged constructs for CDK5, GSK3β, and mitogen-activated protein kinase 1 (MAPK1/ERK2) and an additional set of p25 and p35 with a mCherry-tag. GFP- and mCherry-tagged constructs were cotransfected into cultured primary embryonic (E16.5) mouse neurons grown for 14 d in vitro (DIV14). Consistent with our co-IP results, cotransfection of GFP-tagged GSK3β with mCherry-p25 resulted in highly significant FRET, whereas GFP-GSK3β overexpressed with mCherry-p35 led to no transfer above background (Fig. 1 *C* and *D*). As expected, control cultures in which GFP-CDK5 was overexpressed with mCherry-p25 (or mCherry-p35) displayed significant energy transfer in both cytoplasm and nucleus (Fig. S1*B*). GFP-tagged MAPK1 (ERK2) was used as a negative control because it is also a member of the CMGC kinase family (31); with either p25 or p35 revealed no significant FRET in our assay (Fig. S1*B*, rows 3 and 4). Thus, the interaction we observed between GSK3β and p25 is direct and specific. The results thus far were found in the neuronal cell body. We also examined GSK3β:p25 FRET in distal neurites. Even in this area of the neuron, GSK3β:p25 displayed significant FRET (Fig. 1*D*), as it did with CDK5:p35 and CDK5:p25 (Fig. S1*B*). The negative control, ERK2, produced no FRET signal with either p35 or p25 (Fig. S1*B*). Thus, the interaction between p25 and GSK3β is independent of subcellular localization.

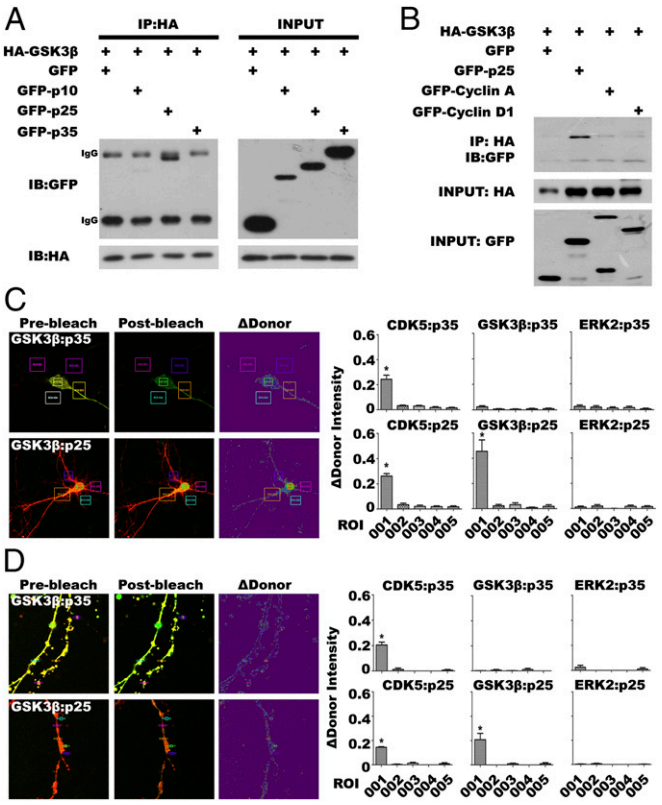

Fig. 1. GSK3β interacts with p25. (*A*) Potential interactions between GSK3β and p35/p25/p10 were detected by co-IP followed by Western blot ($n = 3$ experiments). (*B*) Although cyclin A and cyclin D1 are both similar to p25 structure, co-IP followed by Western blot failed to detect interaction with GSK3β ($n = 3$ experiments). (*C* and *D*) FRET by acceptor photobleaching in DIV14 E16 embryonic neurons cotransfected with GFP-tagged GSK3β/CDK5/ERK2 (donor) and mCherry-tagged p35/p25 (acceptor). Acceptor photobleaching was performed [region of interest (ROI) 001] in the cell body region (*C*; see also Fig. S1*B*) or in the neurites (*D*; see also Fig. S1*B*). To ensure the signals detected were specific, areas without photobleaching (ROI 002–ROI 005) were also analyzed. GFP-CDK5/mCherry-p35 and GFP-CDK5/mCherry-p25 pairs served as positive controls (Fig. S1*B*) (initial magnification 630×). Samples were compared by one-way ANOVA with Bonferroni post hoc test. $^*P < 0.05$ vs. ROI 002–ROI 005 groups; $n = 30$ in three experiments.

p25 Preferably Binds GSK3β Over CDK5. We next sought to determine the relative affinities of the kinases for the p25 and p35 activators in cells overexpressing three proteins. When p35, CDK5, and GSK3β were expressed together, the CDK5:p35 interaction predominated; virtually no GSK3β:p35 binding was observed (Fig. 2*A*, lane 2). When p35 was replaced with p25, however, a CDK5 interaction was present, but GSK3β:p25 predominated (Fig. 2*A*, lane 5). This enhanced affinity for p25 is unique to GSK3β. Overexpression of other CDKs in the presence of p25 plus CDK5 revealed no similar competitive advantage (Fig. 2*B*). These findings suggest that even though it has been cited as a strong CDK5 activator (17), in our model system p25 has a higher affinity for GSK3β than for CDK5.

We next attempted to predict the binding site of p25 on GSK3β. Constructs expressing HA-tagged truncated fragments of GSK3β were cotransfected with GFP-p25 (Fig. 2*C*). Co-IP with anti-HA followed by Western blotting with GFP antibody showed that sequences located at T-loop as well as AXIN-binding channel fragments in C terminus are needed to facilitate the interaction with GFP-p25 (Fig. 2*C*). These observations were less informative than we had hoped, so we also performed in silico docking analyses using ClusPro 2.0 software (cluspro.bu.edu/login.php). Because several lines of evidence suggested the interaction between CDK5 and p25 is predominantly hydrophobic (35, 36), we autosimulated CDK5

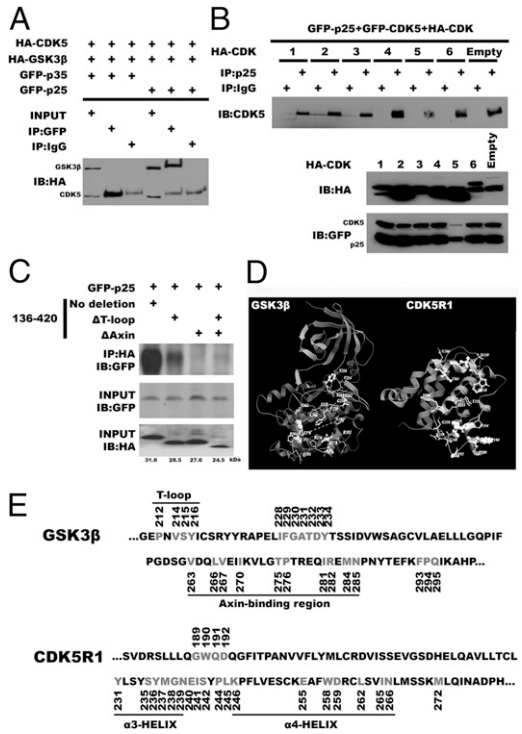

Fig. 2. p25 preferably binds GSK3β over CDK5 and interacts with a different domain of the protein. (*A*) Co-IP and Western blotting experiments show that GSK3β outcompetes CDK5 for interaction with p25 ($n = 3$ experiments). (*B*) CDK5 was coexpressed with other CDKs; none could significantly disrupt the interaction between p25 and CDK5 (compare with *A*; $n = 3$ experiments). (*C*) Truncated fragments of GSK3β were coexpressed with p25 to investigate the site(s) of interaction. Deletion of sequences in the T-loop (ΔT-loop) or AXIN-binding domain (ΔAXIN) resulted in reduced interaction with p25 ($n = 3$ experiments). (*D*) Molecular models of GSK3β (PDB ID code 1Q4L, chain A) and p25 (PDB ID code IUNL, chain D) showing residues involved in interactions, as analyzed by contact area analysis. (*E*) Points of most likely contact are the amino acid residues highlighted in gray.

[Protein Data Bank (PDB) ID code 1UNL, chain A] and p25 (PDB ID code 1UNL, chain D) interaction using a hydrophobic-favored mode. We compared the free energy score of each cluster center because this region is regarded as the representative structure for the cluster (37). For p25 and CDK5, the score of the first ranked cluster conformation was −912.6 kcal/mol (Fig. S2*A*). Notably, when the same criteria were applied to p25 and GSK3β (PDB ID code 1Q4L, chain A), the score of the best cluster conformation was −1,149.9 kcal/mol, suggesting a more favorable binding (Fig. S2*A*).

To further understand how p25 interacts with GSK3β, contact area analysis was performed using ICM-Browser Pro based on the most favorable confirmation obtained from ClusPro 2.0 docking. Unlike the binding modes of CDK5:p25, in which the α3 and α4 helixes of p25 interact and form a wedge between the activation loop (T-loop) and the PSSALRE helix on CDK5 (38), we found that residues from the α3 and α4 helixes of p25 are not only predicted to interact with residues on the GSK3β T-loop, but also heavily with residues within the AXIN-binding channel (Fig. 2 *D* and *E*). Physically, the channel is located in the C-terminal helix (amino acids 262–273) and an extended loop between amino acids 285 and 299 (39). Five intermolecular hydrogen bonds between GSK3β and p25 are predicted that would stabilize the interaction (Fig. S2*B*). Three of these bonds are predicted to involve the arginine at position 278 of GSK3β—one with the methionine at position 237 (predicted bond length = 1.81 Å) and two with the glycine residue at position 238 (predicted bond lengths = 1.94 Å and 2.15 Å; Fig. S2*B*, *Middle*). The fourth predicted hydrogen bond can be found on the GSK3β C-terminal extended loop, between the phenylalanine at position 293 of GSK3β and the tryptophan at position 190 of p25 (1.89 Å; Fig. S2*B*, *Bottom*). In fact, this region of GSK3β is of particular interest because phosphorylation of the nearby tyrosine at position 216 (Y216) can lead to activation of the kinase (40). When the two proteins are associated, Y216 on GSK3β is predicted to form a hydrogen bond with the aspartate residue at position 259 on p25 (1.92 Å; Fig. S2*B*, *Top*). These data, together with the docking results, offer a compelling rationale for the strength of the observed biochemical affinity between GSK3β and p25.

p25 Binding Enhances GSK3β Primed Phosphorylation Activity and Leads to Aberrant Tau Phosphorylation. According to the literature, GSK3β is a serine/threonine kinase that has a unique choice of substrate preference (41); it is one of the few kinases that prefer prior phosphorylation of its substrate before it can further phosphorylate the protein at the "primed" motif: (S/T-XXX-S/T[P]). We next explored the effects of p25 binding on GSK3β kinase activity in vitro. To visualize GSK3β activity in living cells, we used a GFP-GSK3-MAPK reporter (42). DIV14 primary neuronal cultures from wild-type B6 mice were transfected with mCherry-p35 or mCherry-p25, along with the reporter and assayed after 24 h. In the presence of active GSK, the phosphorylation of the marker should lead to a loss of GFP fluorescence in the transfected cells (*Materials and Methods*); this is the result we observed with p25, especially in cells expressing higher levels of mCherry-p25 (Fig. 3*A*, third row, asterisk-marked cell). By contrast, when p35 was transfected, the GFP reporter signal stayed strong in the mCherry-positive cells (Fig. 3*A*, second row); this is the result expected if p35 does not change the activity of GSK3β. The p25 effect on GSK3β kinase activity is independent of CDK5, because we obtained similar results when the same experiment was conducted with DIV14 neurons isolated from E16 embryonic cortex of *Cdk5* knockout mice (Fig. 3*A*, rows 4–6). As further evidence of this model, cells transfected with a phosphorylation-resistant GSK3β reporter protein showed no loss of fluorescence when transfected with either p35 or p25 (Fig. S3*A*).

Unlike other protein kinases, GSK3β is constitutively active in resting conditions and is inhibited in response to cellular signals (43). We found that phosphorylation of the serine 9 (Ser9) residue of Gsk3β was significantly reduced in N2a cells overexpressing p25, suggesting that a blockage of Ser9 phosphorylation might be the cause of the enhanced primed-phosphorylation activity observed with p25 (Fig. 3*B*). Consistent with this suggestion, the intensity of immunostaining for phospho-Gsk3β (Ser9) was found to be significantly reduced in cortices of embryonic brains after induced ectopic expression of p25 by in utero electroporation (Fig. 3*C*) and in mature brains from bitransgenic CK-p25 mice in which the forebrain expression of p25 was induced for 8 wk beginning at 2 mo of age by removal of deoxycycline from drinking water (Fig. 3*D*; for details, see *Materials and Methods*). As a final independent confirmation, we performed stereotactic injection of kainic acid (KA) into the hippocampus. This excitotoxicity model has enhanced cleavage of p35, resulting in elevated levels of p25 (44). Both Western blots and immunohistochemistry with brain tissues isolated from these mice further support the inverse correlation between the levels of p25 protein and phospho-GSK3β (Ser9) (Fig. S3*B*).

Aberrant activity of GSK3β by interaction with p25 may also affect the phosphorylation status of its substrates such as tau, which is implicated in neurodegeneration (45); to test this, N2a cells were transfected with HA-GSK3β and GFP-p35. When the HA immunoprecipitates were assayed for tau kinase activity, we observed little to no tau phosphorylation at sites threonine-181 (Thr181) or serine-396 (Ser396) in vitro. By contrast, in cells overexpressing HA-GSK3β and GFP-p25, the immunoprecipitate demonstrated a modest (twofold) increase in tau phosphorylation at these sites (Fig. 4*A* and Fig. S4*A*). To verify that these observations were a result of aberrant GSK3β activity, tau phosphorylation was measured in p25-expressing N2a cells that

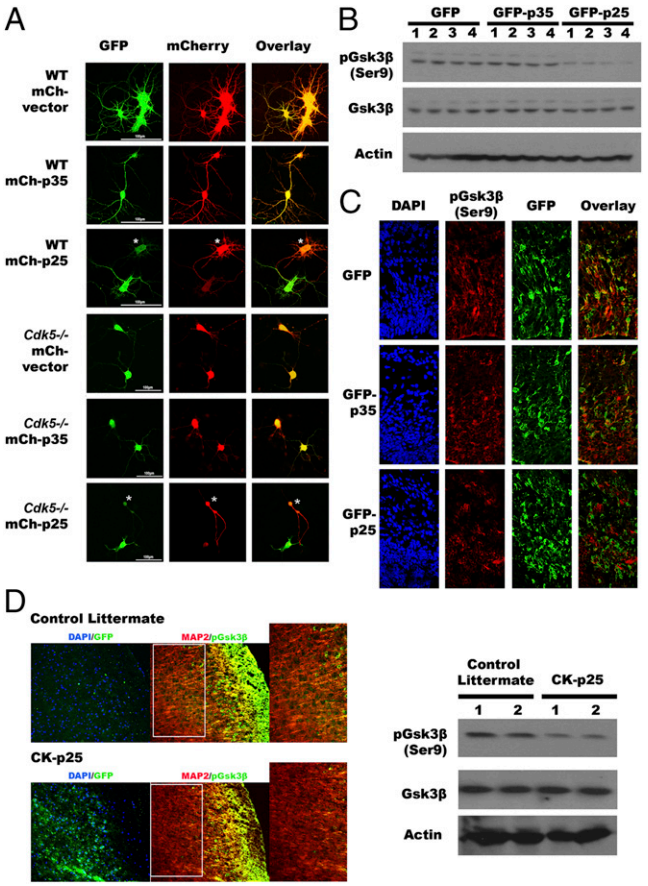

Fig. 3. GSK3β activity is altered by p25, which correlated with a loss of phosphorylation at serine 9. (*A*) The activity of GSK3β was visualized in both wild-type and *Cdk5*$^{-/-}$ DIV14 primary neurons overexpressing p25 or p35, with a GFP-GSK3-wtMAPK reporter. p25 activates Gsk3β in both wild-type and *Cdk5*$^{-/-}$ neurons (15 replications from three independent experiments). (*B–D*) Phosphorylation levels of serine 9 residue on Gsk3β in the presence of p25 were demonstrated by immunoblotting (*B*) and immunohistochemistry (*D*). (*B*) Phosphorylation of serine 9 on Gsk3β was reduced in N2a cells with ectopic expression of p25 but not p35 ($n = 3$ experiments). (*C*) Immunohistochemistry showed introduction of p25 constructs into embryonic cortices by in utero electroporation resulted in reduced levels of phosphorylated Gsk3β at serine 9 ($n = 3$ experiments). (*D*) Cortices of adult transgenic mice with ectopic p25 showed similar results by immunohistochemistry and immunoblotting. Serine 9 phosphorylation was reduced, whereas total Gsk3β level remained similar ($n = 3$ animals in each group).

were also treated with *Cdk5* or *Gsk3β* siRNA. Immunoblotting showed that *Gsk3β* knockdown could significantly reverse the p25 effect on tau phosphorylation level, but only a modest reversal was observed with *Cdk5* knockdown (Fig. 4*B*). The effect of aberrant activity of GSK3β toward tau can also be seen in the brains of various mouse models of Alzheimer's disease in which the levels of p25 have been shown to be increased (46, 47). We harvested brain cortical lysates from mouse models of 3xTg (B6;129-Psen1tm1MpmTg(APPSwe,tauP301L)1Lfa/Mmjax) and its corresponding background control 129S (B6129SF2/J), together with those from PS1/APP (B6.Cg-Tg(APPswe,PSEN1dE9) 85Dbo/Mmjax) mice. Immunoblotting data confirmed that endogenous p25 levels were significantly elevated in aged mice of both 3xTg (12 mo) and PS1/APP models (14 mo) compared with their corresponding controls (Fig. 4*C*). Though the mechanisms leading to elevated p25 likely differ, Western blotting showed that tau phosphorylation at both the PHF1 (Ser396/Ser404) and AT8 (Ser202/Thr205) epitopes was significantly increased (Fig. 4*C*), consistent with our model.

GSK3β:p25 Binding Alters the Stability of β-Catenin by Blocking Formation of the GSK3β/AXIN/APC Complex. It has been reported that tau phosphorylation is accompanied by decreased β-catenin phosphorylation and accumulation of the protein (48). Consistent with this finding, the levels of total β-catenin were dramatically increased in N2a cells overexpressing p25, but not in those overexpressing p35 (Fig. 5*A*). Such increase was not associated with altered transcription (Fig. S4*B*) but was a result of enhanced stability of the β-catenin protein induced by dephosphorylation of Ser33/37/Thr41 (Fig. 5*B*). This effect is most likely based on the actions of Gsk3β in the cytoplasm (Fig. 5*B*, lanes of GFP-p25-NLS). When p25 was directed into the nucleus with a nuclear localization signal (NLS; Fig. 5*B*), phosphorylation of β-catenin returned to a level comparable to controls. Directing p25 to the cytoplasm with a nuclear export signal (NES) was as effective as wild-type p25 in reducing β-catenin phosphorylation. These findings suggest that the cytoplasmic interaction of p25 with GSK3β plays a key role in determining the stability of β-catenin.

β-catenin is recognized part of the canonical WNT signaling pathway. When the WNT receptor (frizzled) is activated, the "destruction complex" composed of GSK3β, AXIN, and APC dissociates (49), and this results in the failure of GSK3β to find

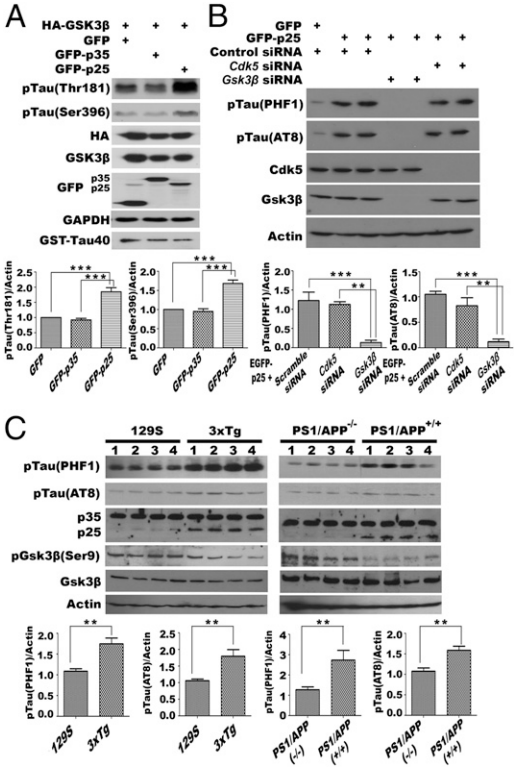

Fig. 4. Tau is aberrantly phosphorylated by GSK3β under the influence of p25. Tau phosphorylation at known GSK3β sites was analyzed in N2a (*A*) (Fig. S4*A*) cells transiently overexpressing GSK3β with p25 or p35. Coincubation of Tau40 proteins with lysates from GSK3β and p25 cotransfected cells resulted in elevated levels of phosphorylation ($n = 3$ experiments). (*B*) Phosphorylation of tau at PHF1 and AT8 sites were reversed in p25-overexpressing N2a cells having *Gsk3β* presilenced. Quantifications of the relative pTau/Actin intensities are shown ($n = 3$ experiments). (*C*) Brain cortex lysate from two mouse AD models and their appropriate controls: 129S vs. 3xTg (12 mo); PS1/APP$^{-/-}$ (wild type) vs. PS1/APP$^{+/+}$ (both 14 mo old) were probed for the levels of p25, as well as phosphorylation of tau at PHF-1 and AT8 epitopes. Quantifications of relative pTau/Actin intensities are shown ($n = 3$ experiments). Statistical analyses between two groups were compared by Student *t* test, and those between three groups were compared by one-way ANOVA with Bonferroni post hoc test. $^{**}P = 0.001$; $^{***}P < 0.001$.

its β-catenin substrate, blocking catenin phosphorylation and preventing its targeting to the proteasome for degradation. Because our docking data predicted that the p25 interaction site on GSK3β is located within the AXIN-binding channel (Fig. 2 *C–E*), we speculated that the loss of β-catenin phosphorylation might be caused by the breakup of the AXIN/APC/GSK3β complex. Support for this hypothesis comes from comparing co-IP assays with and without ectopic expression of GFP-p25 in N2a cells. The presence of exogenous p25 blocked the physical interactions between Gsk3β with both Axin and Apc (Fig. 5*C*). A similar loss of the Axin/Apc/Gsk3β complex was also observed in brain cortical lysates from the two AD mouse models (Fig. 5*D*). These observations suggest that p25 interaction with GSK3β hinders the formation of the AXIN/APC/GSK3β destructive complex both in vivo and in vitro, leading to reduced β-catenin phosphorylation.

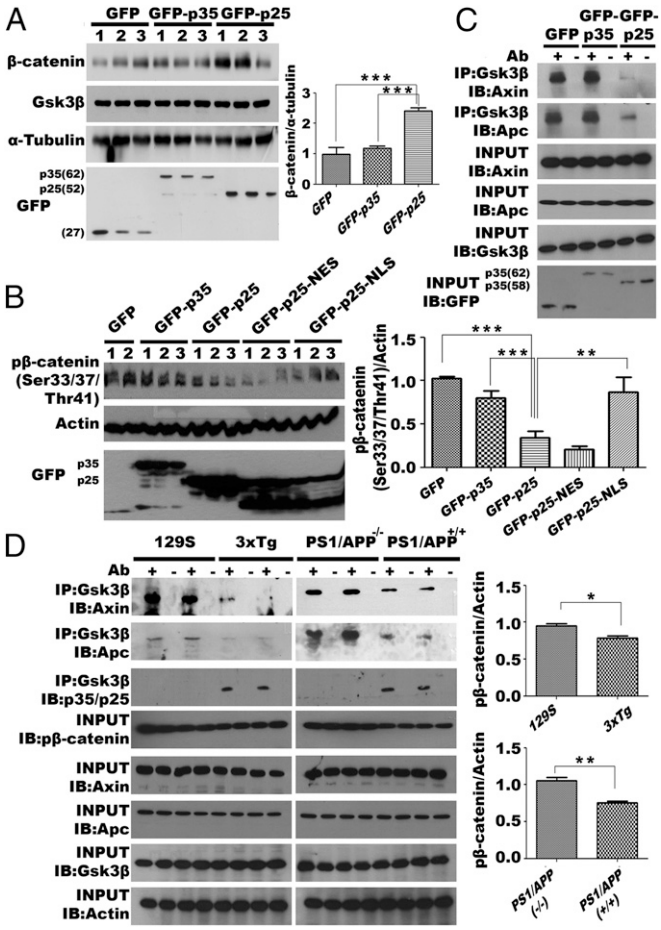

Fig. 5. Phosphorylation of β-catenin is reduced when p25 interacts with GSK3β and hinders the formation of cytosolic GSK3β/AXIN/APC β-catenin destructive complex. (*A*) Total level β-catenin was detected in N2a cells transiently expressing GFP-p35, GFP-p25, or GFP control by Western blotting. Ectopic expression of p25 resulted in elevated levels of total β-catenin ($n = 3$ experiments). Quantification of relative β-catenin/tubulin level is shown to the right of the blots. (*B*, *Left*) Levels of phospho-β-catenin (S33/S37/T41) were detected in N2a cells overexpressing p25, nuclear-p25 (p25-NLS), and cytoplasmic p25 (p25-NES) ($n = 3$ experiments). (*Right*) Quantification of relative phospho-β-catenin/Actin level. (*C*) Axin and Apc interaction with Gsk3β in N2a cells overexpressing p35 or p25 was analyzed by co-IP and Western blotting ($n = 3$ experiments). (*D*, *Left*) Reduced phosphorylation of β-catenin and loss of interaction among Gsk3β, Axin, and Apc were also observed in 3xTg (12 mo) and PS1/APP ($^{+/+}$) (14 mo), compared with corresponding controls ($n = 3$ experiments). (*Right*) Quantification of relative phospho-β-catenin/actin level.

GSK3β:p25 Triggers Neurite Collapse and Presynaptic Loss. We ectopically expressed GFP-CDK5, -GSK3β, or -ERK2 with either mCherry-p35 or -p25 in DIV14 primary cortical neurons and quantified the neuritic morphology of the challenged cells (Fig. 6). Coexpression of p25 with CDK5, GSK3β, or ERK2 resulted in a diminished number of neurites compared with cells transfected with only of the three kinases, and the pairwise comparisons with *t* test indicated that the differences observed between GSK3β and GSK3β:p25 groups were statistically significant (Fig. 6*B*). More importantly, coexpression of GSK3β:p25 resulted in a more dramatic loss of neurites than CDK5:p25. Consistent with previous reports (17), we found that introduction of p25 plus CDK5 into cultured primary neurons induced neurite loss, although p35 plus CDK5 was almost equally destructive. By far the greatest damage, however, was seen in primary neurons overexpressing p25 plus GSK3β (Fig. 6), and was significantly worse than that induced by p25 plus CDK5. Consistent with previous findings (22, 50), our data therefore suggests aberrant activity of GSK3β can also lead to loss of neurite arborization.

The GSK3β:p25 induced neurotoxicity, was confirmed in cultured neurons by the reduction in staining intensity for the presynaptic marker synapsin-I. As expected, we observed a significant reduction in the density of puncta (defined as overlap of synapsin-I and fluorescent marker staining of the transfected cells) in primary neurons coexpressing GFP-CDK5 plus mCherry-p25. Intriguingly, overexpression of p25 alone induced an even more significant synaptic loss than that seen when it was coexpressed with CDK5, which suggests that the inclusion of CDK5 partially buffered the effects triggered by p25 alone (Fig. 7 *A* and *B*). The significance of this finding was further enhanced by our observation that primary neurons coexpressing p25 plus GSK3β suffered the most dramatic synaptic loss of all (Fig. 7 *A* and *B*). Using in utero electroporation, we produced similar results in the neurons of the embryonic mouse cortex (Fig. 8 *A* and *B*). In this case, however, the density of postsynaptic puncta (defined as overlap of PSD95 and fluorescent marker staining of transfected cells), revealed no significant changes among the treatments (Fig. S5).

We confirmed the GSK3β dependence of this effect by using specific siRNA against *Cdk5* or *Gsk3β*. Cells were pretreated with siRNA for 24 h followed by transfection of GFP-p25 for another 24 h prior to fixation. Treatment with *Cdk5* siRNA resulted in modest improvement in both neuritic morphology and synaptic density in cells expressing p25 (Fig. 9 *A*, *C*, and *D*). In cultures pretreated with *Gsk3β* siRNA, however, the improvements in these two parameters were far more substantial (Fig. 9 *B–D*). Collectively, our data provided evidence that p25-activated GSK3β is a significant part of the pathological impact on neurons when p25 levels are elevated.

Discussion

CDK5 and GSK3β have both been proposed to play a pathogenic role in AD, in large part by contributing to the hyperphosphorylation of tau, one of the pathological hallmarks of the disease. GSK3β has been shown to colocalize with dystrophic neurites and neurofibrillary tangles (51, 52). Active GSK3β appears in neurons with pretangle changes (28), and increased activity is detected in frontal cortex (53) and hippocampus (54) of AD patients. In the present study, we report that p25, a well-known coactivator of CDK5, interacts with GSK3β by directly binding to its T-loop and AXIN-binding channel. The affinity of p25 for GSK3β is higher than for CDK5, and p25 binding aberrantly activates GSK3β and alters its substrate specificity. In vitro, GSK3β:p25 is highly neurotoxic; both neurite arborization and the density of synaptic puncta are significantly reduced in primary neurons. The effect is GSK3β-specific, because treatment of cells with *Gsk3β* siRNA can block these toxic effects. Treatment with siRNA against *Cdk5*, by contrast, is without significant effect.

The CMPK family kinases share strong structural homologies with each other, and these similarities are not restricted to the

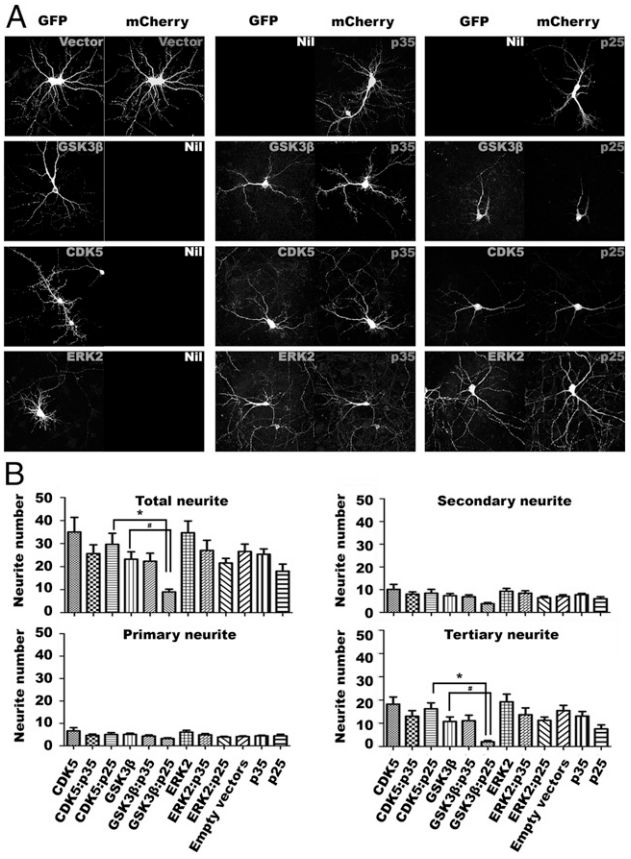

Fig. 6. GSK3β:p25 triggers neurite collapse in primary neuronal culture. Morphologies of E16 embryonic primary neurons at DIV14 cotransfected with GFP-tagged GSK3β, CDK5, or ERK2 in GFP-IRES vectors and p35 or p25 in mCherry-IRES vectors were analyzed. (*A*) Representative images of primary neurons showing changes in neurite morphology upon ectopic expression of the indicated constructs after 24 h. Ectopic GSK3β and p25 coexpression resulted in the most severe loss of neurites of primary cortical neurons (total $n = 30$ from three experiments). (*B*) Quantitative analysis of the total number of neurites, and subanalysis of primary, secondary, and tertiary neurites among different treatment groups ($^{*}P < 0.05$, with all groups of samples were compared by one-way ANOVA with Bonferroni post hoc test. $^{\#}P < 0.005$ between GSK3β and GSK3β:p25 by Student *t* test; $n = 30$ from three experiments.

kinase domain, as can be seen in Fig. S1*A*. Given that CDK5 is capable of binding traditional cyclins as well as its own cyclin-like proteins—p35 and p39—we reasoned that GSK3β might also have residual cyclin binding activity. This hypothesis proved incorrect; despite our initial ideas, the homology of GSK3β does not extend to its ability to bind cyclins. In searching for evolutionary conservation, however, we discovered an unexpected relationship between the p25 breakdown product of p35 and GSK3β. Other CDK family members can bind multiple cyclins, though they are typically activated by specific ones (55). GSK3β, by contrast, shows a high specificity for p25, likely due largely to the fact that rather than binding in the typical cyclin pocket, p25 interacts with the AXIN-binding domain. This structural conclusion is supported by the analysis performed using ClusPro 2.0 software and by the disruption by p25 of the physical interaction of the proteins of the AXIN/APC/GSK3β complex.

Although there is conflicting evidence on whether p25 levels are elevated in AD, there is clear evidence that exogenous Aβ is able to increase p25 production in neurons (56). Further, mice that conditionally overexpress p25 show synaptic loss and learning deficits (57). The traditional view of these data assumes that p25 exerts its effects by interaction with CDK5 (56). Our data suggest a reexamination of this assumption is needed, however, and a potential role of GSK3β should also be considered. The in vitro data forms a significant part of this argument—in particular, the demonstration that knockdown of *Gsk3β* with siRNA is much more effective at blocking the p25-induced neurodegeneration than is the *Cdk5* siRNA. The in vivo data deserve special consideration, however, because they carry important implications for the etiology of various neurodegenerative conditions.

Our data show that overexpression of p25 in vivo as well as in vitro drives tau hyperphosphorylation (Fig. 4 and Fig. S4) accompanied by a severe loss of neurites and presynaptic puncta (Figs. 7 and 8). These findings are in accord with earlier results, but extend them considerably. Though earlier findings were logically interpreted as reflecting the interaction of the exogenous p25 with CDK5, our data demonstrate that p25 elevation in vivo, whether caused directly by the expression of a p25 transgene or indirectly by the altered environment of human APP overexpression, leads to the increased appearance of hyperphosphorylated tau. What our data also show, however, is that elevated p25 in vivo is also associated with evidence for enhanced GSK3β activity, as reflected by decrease in protein phosphorylation level.

Our present findings demonstrate that in the presence of p25, both CDK5 and GSK3β are activated. Evidence from the PC12 cell line suggests that AKT binds to the AXIN:GSK3β complex and phosphorylates GSK3β at serine 9, reducing its activity (58).

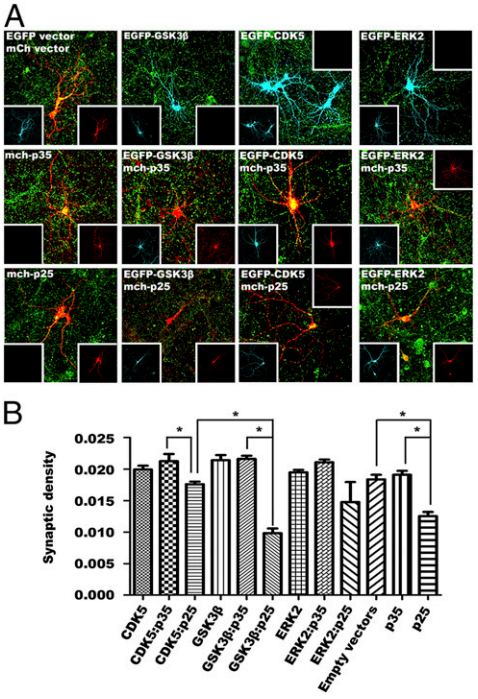

Fig. 7. GSK3β:p25 triggers synaptic loss in primary neuronal culture. Synaptic densities of E16 embryonic primary neurons at DIV14 transfected with GFP-tagged GSK3β in GFP-IRES vector and or without p35 or p25 in mCherry-IRES were analyzed. (*A*) Representative images of primary neurons with presynaptic staining responding to ectopic expression of different constructs for 24 h were shown (cyan, GFP; red, mCherry; green, synapsin-I). Ectopic GSK3β and p25 coexpression resulted in the most severe loss of presynaptic puncta in these primary cortical neurons (total $n = 30$ from three experiments). (*B*) Quantitative analysis of the density of presynaptic puncta (overlapping of green fluorescent puncta with red of transfected cell dendrite, divided by the total number of pixels of each cell) among different treatment groups. Samples were compared by one-way ANOVA with Bonferroni post hoc test. $^{*}P < 0.05$; $n = 30$ from three experiments.

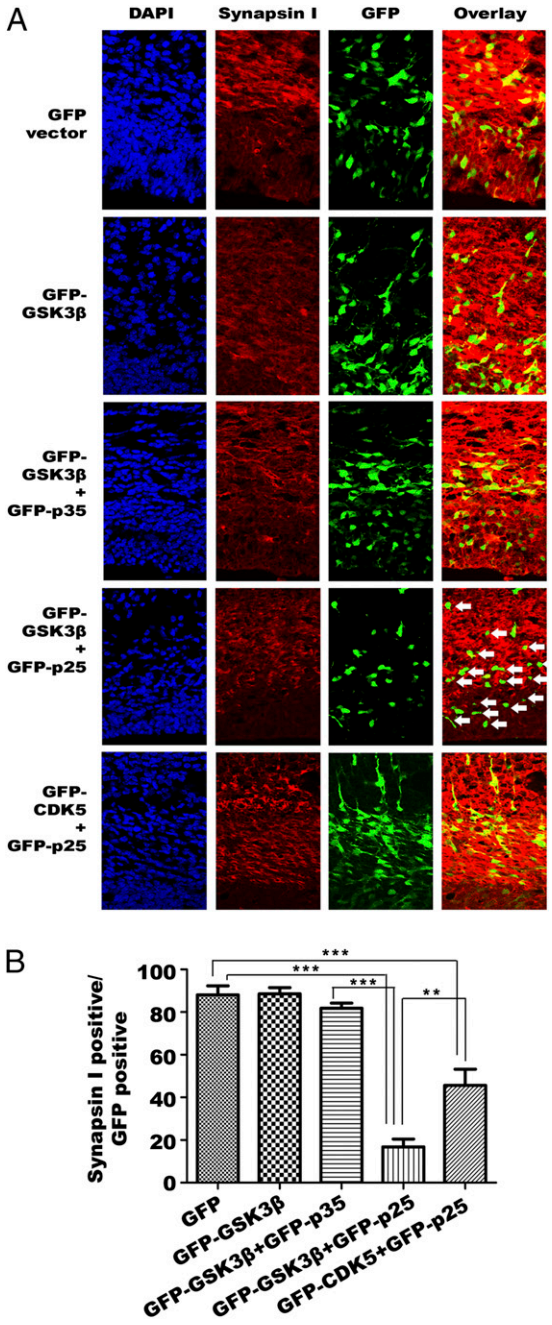

Fig. 8. GSK3β:p25 triggers synaptic loss in embryonic cortex. Synaptic density of embryonic sections from the cortex of embryos transfected with GFP-tagged p25/p35 with or without GFP-tagged GSK3β or CDK5 by in utero electroporation. (*A*) Representative images of cortical sections with presynaptic staining in response to ectopic expression of different constructs. GSK3β and p25 coexpression resulted in the most severe loss of neurites (tails of neurons) and presynaptic signals (overlap between GFP and synapsin-1) in cortex (n = 3 experiments). White arrows indicate the GSK3β and p25 coexpressing neurons (*B*) Quantitative analysis of the percentage of synapsin I positive GFP-positive cells (number of GFP-positive cells with positive red synapse in signals, divided by the total number of total GFP-positive cells) among different treatment groups. Samples were compared by one-way ANOVA with Bonferroni post hoc test. $^{**}P = 0.001$; $^{***}P < 0.001$.

Combined with our data showing that GSK3β preferentially binds to p25 over AXIN, we speculate that p25 binding may prevent GSK3β from being inhibited by AKT-mediated phosphorylation. Our Western blotting results reveal the levels of phosphorylated serine 9 on GSK3β are substantially reduced in the presence of p25, both in vitro in cycling N2a cells and in vivo in neurons (Fig. 3 *B–D*). Our data suggest that of the two kinases, p25 has a higher affinity for GSK3β than for CDK5, which would imply that p25 preferentially alters the activity of GSK3β. In support of this, we observed that neurons co-overexpressing GSK3β and p25 show severe neurodegeneration—more severe than those overexpressing p25 alone. Indeed, co-overexpression of CDK5 with p25 in nerve cells is somewhat protective and leads to the mildest phenotype of all (Figs. 6–8 and Fig. S5).

Our data add to the appreciation that there is substantial cross-talk between the CDK5 and GSK3β kinases. In this vein, we find it noteworthy that CDK5 is able to phosphorylate AXIN at threonine 485. Phosphorylated AXIN binds to GSK3β and inhibits its activity, leading the authors of this study to suggest that CDK5 serves as a modulating influence and, through its targeting of AXIN, functions normally to prevent GSK3β overactivation (58). In conjunction with the data presented here, however, we would speculate that in the presence of p25, this interaction is blocked (Fig. 5 *C* and *D*). GSK3β is no longer under inhibitory regulation and thus becomes aberrantly activated. This model is consistent with our gene knockdown studies showing that inhibition of GSK3β is far more effective than inhibition of CDK5 in blocking the neurite and synapse loss following p25 expression.

We propose that in most in vivo situations, the action of p25 is twofold; it alters both GSK3β and CDK5 activities. In healthy mature postmitotic neurons, nuclear CDK5 suppresses the reentrance into the cell cycle by forming a complex with p35 and E2F1 (13, 59). Enriched neuronal p25 in disease conditions may act as a competitor of p35-E2F1, and eventually prevent CDK5 from suppressing the cell cycle inside the nucleus. At the same time, our data show that β-catenin is stabilized in the presence of p25. We consider it plausible that these elevated levels of β-catenin may lead to its interaction with non-GSK3β bound

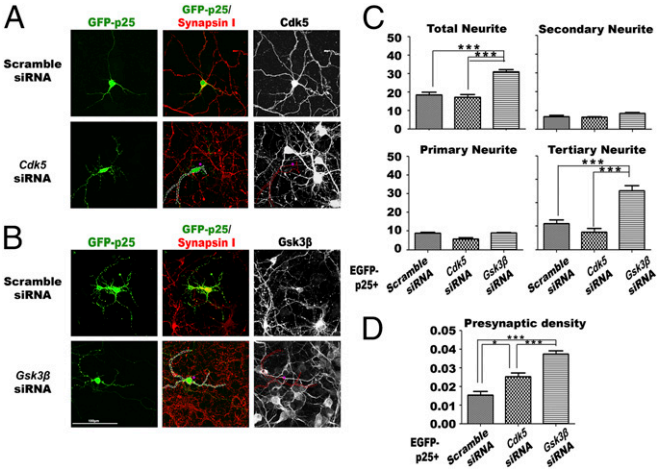

Fig. 9. GSK3β knockdown blocks the degenerative effect of p25. Morphologies of E16 embryonic primary neurons at DIV14 that had been pretreated for 24 h with scrambled siRNA, siRNA against *Cdk5*, or siRNA against *Gsk3β*, followed by transfection with p25 in an mCherry-IRES vector for another 24 h. (*A* and *B*) Representative images of primary neurons with various degrees of changes in neurite morphology upon different treatments. Pretreatment of cells with siRNA against *Gsk3β* abolished the destructive effect on neurites and synapses triggered by ectopic expression of p25 (total n = 30 from three experiments). (*C*) Quantitative analysis of the total number of neurites, and subanalysis of primary, secondary, and tertiary neurites. (*D*) Differences in presynaptic density among the different treatment groups. $^{*}P < 0.05$; $^{**}P = 0.001$; $^{***}P < 0.001$, all groups of samples compared by one-way ANOVA with Bonferroni post hoc test; n = 30 from three experiments.

phosphorylated-AXIN and thus become activated inside the nucleus (60). Whether β-catenin activity in the postmitotic mature neurons serves as antiapoptotic force or eventually drives the cells to reenter the cell cycle awaits additional studies. Our results provide a new direction for future studies on p25- and GSK3β-mediated neuronal atrophy associated with the pathophysiological mechanisms underlying Alzheimer's and other neurodegenerative diseases.

Materials and Methods

Animal Maintenance, Cortical Brain Tissue Isolation, and Primary Neuronal Culture. C57BL/6J, 3xTg-AD [B6;129-Psen1^{tm1Mpm}Tg(APPSwe,tauP301L)1Lfa/Mmjax], and PS1/APP [B6C3-Tg(APPswe,PSEN1dE9)85Dbo/Mmjax] mice obtained from Jackson Laboratory; colonies of C57BL/6-Tg(tetO-p25/GFP)337Lht/J are generous gifts from Li-Huei Tsai, Massachusetts Institute of Technology, Cambridge, MA, and B6;129-Cdk5^{tm1Kul}/J is a generous gift from Nancy Yuk-Yu IP, Hong Kong University of Science and Technology, Hong Kong, were maintained and bred in the Animal and Plant Care Facility of The Hong Kong University of Science and Technology (HKUST). A colony of *Cdk5*$^{-/-}$mice was maintained on a mixed (C57BL/6J X 129/S1) background and bred in the Animal Core Facility of Xiamen University. All animal experimental protocols were approved both by the Animal Ethics Committee at HKUST (and their care was in accord with the institutional and Hong Kong guidelines) and by the Xiamen University Institutional Animal Care and Use Committee. Cortical brain tissue and embryonic cortical neurons were isolated by standard procedures as reported previously (12).

FRET–Acceptor Photobleaching. Primary neuronal culture at DIV12–13 cultured in a 35-mm glass-bottom culture dish (MatTek Corporation) were cotransfected with two constructs (GFP-GSK3β/GFP-CDK5/GFP-ERK2 or mCherry-p25/mCherry-p35) using Lipofectamine LTX with Plus Reagent (Life Technologies) as described. After incubation for 24 h, cell images in the green and red channels were acquired, and FRET-AB analysis was performed using a TCS Sp8 confocal microscope (Leica Microsystems Inc.).

Immunocytochemistry and Immunohistochemistry. For immunostaining, N2a cells and primary neuronal cultures were grown on 13-mm coverslips (Marienfeld) in 24-well plates, Twenty-four hours after transfection (with or without treatment), cells were harvested, fixed with fresh 4% (wt/vol) paraformaldehyde (Sigma-Aldrich) for 10 min, and permeabilized by treatment with 0.3% Triton X-100 in PBS for 10 min. After blocking with 5% (wt/vol) BSA in PBS for 1 h (blocking solution), primary antibodies were added and incubated overnight at 4 °C. Coverslips were washed 10 min three times with PBS, and secondary antibodies applied for 1 h at room temperature. After three additional washes with PBS, coverslips were mounted with ProLong Gold Antifade Reagent (Life Technologies). Immunofluorescence was analyzed and Z-stacked maximum projected images were photographed using a TCS Sp8 confocal microscope (Leica Microsystems Inc.).

For neurite arborization and synapse quantification in Figs. 8 and 9, constructs that cloned into either pLVX-TRE3G-ZsGreen1 or pLVX-TRE3G-mCherry vectors were used, because the presence of an internal ribosome entry site (IRES) allows coexpression of heterologous gene products (i.e., gene of interest and fluorophore tag) by a message from a single promoter; therefore, localization of the fluorophore protein is independent to the localization of the protein derived from inserts. Z-stacked maximum projected images were used for all counting. Quantification and related statistical analyses were performed blind using ImageJ (NIH) and Photoshop CS6 (Adobe Systems Inc.). For immunohistochemistry, antigens on cryosections were first unmarked with heated citrate buffer at 95 °C for 15 min followed by cooling down at room temperature for 1 h. Sections were rinsed in PBS, blocked with 5% (vol/vol) donkey serum/PBS for 1 h, and immunostained according to the above protocol.

In Silico Automated Protein–Protein Docking and Contact Area Analysis. Docking of ligand protein to receptor protein, energy filtering, clustering, and ranking were done using the ClusPro 2.0 web server (cluspro.bu.edu/login.php) (37, 61). Structures of GSK3β (PDB ID code 1Q4L, chain A), p25 (PDB ID code 1UNL, chain D), and CDK5 (PDB ID code 1UNL, chain A) were obtained from Protein Data Bank to perform docking. As a positive control, we simulated CDK5 and p25 interaction with ClusPro 2.0 using hydrophobic-favored mode, and the same set of parameters were used to simulate the interaction between GSK3β and p25. Representative structures for the cluster were obtained from each simulation, and docking energy center scores of the first ranked cluster conformation were compared. For contact area analysis, ICM-Browser Pro (Molsoft) was used to analyze the key interacting residues and potential presence of interacting bonds of the most favorable confirmation obtained from ClusPro 2.0 docking.

For more experimental details, please see *SI Materials and Methods*.

ACKNOWLEDGMENTS. We thank Prof. Edward De Robertis (University of California, Los Angeles) for sharing the reporter constructs for measuring GSK3β activity, Prof. Li-Huei Tsai (Massachusetts Institute of Technology) for sharing the GFP-p25 transgenic mice [C57BL/6-Tg(tetO-p25/GFP)337Lht/J], and Prof. Nancy Yuk-Yu IP (Hong Kong University of Science and Technology) for sharing the CDK5 knockout mice (B6;129-Cdk5^{tm1Kul}/J). We thank Mr. Jenkin Chan, Mr. Thomas Hui, Ms. Aifang Cheng, Mr. Yang Zhang, Ms. Xuting Shen, Ms. Beika Zhu, and Ms. Toni Man (Hong Kong University of Science and Technology) for their efforts in preparing primary neuronal culture and for routine laboratory support. We also thank Mr. Samuel Lai (Imperial College London), who volunteered as a summer student and assisted in the blinded counting of neurites and synaptic punctas, and Mr. Bob Tang (Leica Microsystems Hong Kong) for his tireless help in providing regular technical training and support. This work was supported by the 985 Project from Xiamen University (J.Z.), National Key Basic Research Program of China Grant 2013CB530900 (to K.H.), National Science Foundation in China Grant 81271421 (to J.Z.), Natural Science Foundation of Fujian Province Grants 013J01147 and 2014J06019 (to J.Z.), the Hong Kong University of Science and Technology, and the Program for New Century Excellent Talents in University (J.Z.). Support for the early phases of this work was provided by National Institutes of Health Grant NS20591 and Rutgers University.

1. Ashford JW (2004) APOE genotype effects on Alzheimer's disease onset and epidemiology. *J Mol Neurosci* 23(3):157–165.
2. Budson AE, Price BH (2005) Memory dysfunction. *N Engl J Med* 352(7):692–699.
3. Terry RD, Peck A, DeTeresa R, Schechter R, Horoupian DS (1981) Some morphometric aspects of the brain in senile dementia of the Alzheimer type. *Ann Neurol* 10(2):184–192.
4. Lee VM, Goedert M, Trojanowski JQ (2001) Neurodegenerative tauopathies. *Annu Rev Neurosci* 24:1121–1159.
5. Terry RD, et al. (1991) Physical basis of cognitive alterations in Alzheimer's disease: Synapse loss is the major correlate of cognitive impairment. *Ann Neurol* 30(4): 572–580.
6. DeKosky ST, Scheff SW (1990) Synapse loss in frontal cortex biopsies in Alzheimer's disease: Correlation with cognitive severity. *Ann Neurol* 27(5):457–464.
7. Cruz JC, et al. (2006) p25/cyclin-dependent kinase 5 induces production and intraneuronal accumulation of amyloid beta in vivo. *J Neurosci* 26(41):10536–10541.
8. Baum L, Hansen L, Masliah E, Saitoh T (1996) Glycogen synthase kinase 3 alteration in Alzheimer disease is related to neurofibrillary tangle formation. *Mol Chem Neuropathol* 29(2-3):253–261.
9. Dhavan R, Tsai LH (2001) A decade of CDK5. *Nat Rev Mol Cell Biol* 2(10):749–759.
10. Tang X, et al. (2005) Cyclin-dependent kinase 5 mediates neurotoxin-induced degradation of the transcription factor myocyte enhancer factor 2. *J Neurosci* 25(19): 4823–4834.
11. Smith DS, Greer PL, Tsai LH (2001) Cdk5 on the brain. *Cell Growth Differ* 12(6):277–283.
12. Cicero S, Herrup K (2005) Cyclin-dependent kinase 5 is essential for neuronal cell cycle arrest and differentiation. *J Neurosci* 25(42):9658–9668.
13. Zhang J, et al. (2008) Nuclear localization of Cdk5 is a key determinant in the postmitotic state of neurons. *Proc Natl Acad Sci USA* 105(25):8772–8777.
14. Turner NC, et al. (2008) A synthetic lethal siRNA screen identifying genes mediating sensitivity to a PARP inhibitor. *EMBO J* 27(9):1368–1377.
15. O'Hare MJ, et al. (2005) Differential roles of nuclear and cytoplasmic cyclin-dependent kinase 5 in apoptotic and excitotoxic neuronal death. *J Neurosci* 25(39):8954–8966.
16. Zhang J, et al. (2010) Cdk5 suppresses the neuronal cell cycle by disrupting the E2F1-DP1 complex. *J Neurosci* 30(15):5219–5228.
17. Patrick GN, et al. (1999) Conversion of p35 to p25 deregulates Cdk5 activity and promotes neurodegeneration. *Nature* 402(6762):615–622.
18. Ahlijanian MK, et al. (2000) Hyperphosphorylated tau and neurofilament and cytoskeletal disruptions in mice overexpressing human p25, an activator of cdk5. *Proc Natl Acad Sci USA* 97(6):2910–2915.
19. Wen Y, et al. (2008) Interplay between cyclin-dependent kinase 5 and glycogen synthase kinase 3 beta mediated by neuregulin signaling leads to differential effects on tau phosphorylation and amyloid precursor protein processing. *J Neurosci* 28(10): 2624–2632.
20. Hooper C, Killick R, Lovestone S (2008) The GSK3 hypothesis of Alzheimer's disease. *J Neurochem* 104(6):1433–1439.
21. Hur EM, Zhou FQ (2010) GSK3 signalling in neural development. *Nat Rev Neurosci* 11(8):539–551.
22. Kim YT, Hur EM, Snider WD, Zhou FQ (2011) Role of GSK3 signaling in neuronal morphogenesis. *Front Mol Neurosci* 4:48.
23. Alabed YZ, Pool M, Ong Tone S, Sutherland C, Fournier AE (2010) GSK3 beta regulates myelin-dependent axon outgrowth inhibition through CRMP4. *J Neurosci* 30(16): 5635–5643.
24. Peineau S, et al. (2008) The role of GSK-3 in synaptic plasticity. *Br J Pharmacol* 153(Suppl 1):S428–S437.

25. O'Brien WT, et al. (2004) Glycogen synthase kinase-3beta haploinsufficiency mimics the behavioral and molecular effects of lithium. *J Neurosci* 24(30):6791–6798.
26. Hughes K, Nikolakaki E, Plyte SE, Totty NF, Woodgett JR (1993) Modulation of the glycogen synthase kinase-3 family by tyrosine phosphorylation. *EMBO J* 12(2): 803–808.
27. Rubinfeld B, et al. (1996) Binding of GSK3beta to the APC-beta-catenin complex and regulation of complex assembly. *Science* 272(5264):1023–1026.
28. Pei JJ, et al. (1999) Distribution of active glycogen synthase kinase 3beta (GSK-3beta) in brains staged for Alzheimer disease neurofibrillary changes. *J Neuropathol Exp Neurol* 58(9):1010–1019.
29. Plattner F, Angelo M, Giese KP (2006) The roles of cyclin-dependent kinase 5 and glycogen synthase kinase 3 in tau hyperphosphorylation. *J Biol Chem* 281(35): 25457–25465.
30. Guidato S, McLoughlin DM, Grierson AJ, Miller CC (1998) Cyclin D2 interacts with cdk-5 and modulates cellular cdk-5/p35 activity. *J Neurochem* 70(1):335–340.
31. Manning G, Whyte DB, Martinez R, Hunter T, Sudarsanam S (2002) The protein kinase complement of the human genome. *Science* 298(5600):1912–1934.
32. Mazanetz MP, Fischer PM (2007) Untangling tau hyperphosphorylation in drug design for neurodegenerative diseases. *Nat Rev Drug Discov* 6(6):464–479.
33. Lacy ER, et al. (2005) Molecular basis for the specificity of p27 toward cyclin-dependent kinases that regulate cell division. *J Mol Biol* 349(4):764–773.
34. Ponsioen B, et al. (2004) Detecting cAMP-induced Epac activation by fluorescence resonance energy transfer: Epac as a novel cAMP indicator. *EMBO Rep* 5(12): 1176–1180.
35. Tang D, Chun AC, Zhang M, Wang JH (1997) Cyclin-dependent kinase 5 (Cdk5) activation domain of neuronal Cdk5 activator. Evidence of the existence of cyclin fold in neuronal Cdk5a activator. *J Biol Chem* 272(19):12318–12327.
36. Chou KC, Watenpaugh KD, Heinrikson RL (1999) A model of the complex between cyclin-dependent kinase 5 and the activation domain of neuronal Cdk5 activator. *Biochem Biophys Res Commun* 259(2):420–428.
37. Comeau SR, Gatchell DW, Vajda S, Camacho CJ (2004) ClusPro: A fully automated algorithm for protein–protein docking. *Nucleic Acids Res* 32(web server issue): W96–99.
38. Tarricone C, et al. (2001) Structure and regulation of the CDK5-p25(nck5a) complex. *Mol Cell* 8(3):657–669.
39. Dajani R, et al. (2003) Structural basis for recruitment of glycogen synthase kinase 3beta to the axin-APC scaffold complex. *EMBO J* 22(3):494–501.
40. Weihl CC, et al. (1999) Mutant presenilin-1 induces apoptosis and downregulates Akt/PKB. *J Neurosci* 19(13):5360–5369.
41. ter Haar E, et al. (2001) Structure of GSK3beta reveals a primed phosphorylation mechanism. *Nat Struct Biol* 8(7):593–596.
42. Taelman VF, et al. (2010) Wnt signaling requires sequestration of glycogen synthase kinase 3 inside multivesicular endosomes. *Cell* 143(7):1136–1148.
43. Farago M, et al. (2005) Kinase-inactive glycogen synthase kinase 3beta promotes Wnt signaling and mammary tumorigenesis. *Cancer Res* 65(13):5792–5801.
44. Crespo-Biel N, Camins A, Canudas AM, Pallàs M (2010) Kainate-induced toxicity in the hippocampus: Potential role of lithium. *Bipolar Disord* 12(4):425–436.
45. Goedert M (2004) Tau protein and neurodegeneration. *Semin Cell Dev Biol* 15(1): 45–49.
46. Kitazawa M, Oddo S, Yamasaki TR, Green KN, LaFerla FM (2005) Lipopolysaccharide-induced inflammation exacerbates tau pathology by a cyclin-dependent kinase 5-mediated pathway in a transgenic model of Alzheimer's disease. *J Neurosci* 25(39): 8843–8853.
47. Green KN, et al. (2008) Nicotinamide restores cognition in Alzheimer's disease transgenic mice via a mechanism involving sirtuin inhibition and selective reduction of Thr231-phosphotau. *J Neurosci* 28(45):11500–11510.
48. Li HL, et al. (2007) Phosphorylation of tau antagonizes apoptosis by stabilizing beta-catenin, a mechanism involved in Alzheimer's neurodegeneration. *Proc Natl Acad Sci USA* 104(9):3591–3596.
49. Clevers H, Nusse R (2012) Wnt/β-catenin signaling and disease. *Cell* 149(6):1192–1205.
50. Seira O, et al. (2010) Neurites regrowth of cortical neurons by GSK3beta inhibition independently of Nogo receptor 1. *J Neurochem* 113(6):1644–1658.
51. Yamaguchi H, et al. (1996) Preferential labeling of Alzheimer neurofibrillary tangles with antisera for tau protein kinase (TPK) I/glycogen synthase kinase-3 beta and cyclin-dependent kinase 5, a component of TPK II. *Acta Neuropathol* 92(3):232–241.
52. Pei JJ, et al. (1997) Distribution, levels, and activity of glycogen synthase kinase-3 in the Alzheimer disease brain. *J Neuropathol Exp Neurol* 56(1):70–78.
53. Leroy K, Yilmaz Z, Brion JP (2007) Increased level of active GSK-3beta in Alzheimer's disease and accumulation in argyrophilic grains and in neurones at different stages of neurofibrillary degeneration. *Neuropathol Appl Neurobiol* 33(1):43–55.
54. Blalock EM, et al. (2004) Incipient Alzheimer's disease: Microarray correlation analyses reveal major transcriptional and tumor suppressor responses. *Proc Natl Acad Sci USA* 101(7):2173–2178.
55. Malumbres M, Barbacid M (2005) Mammalian cyclin-dependent kinases. *Trends Biochem Sci* 30(11):630–641.
56. Lee MS, et al. (2000) Neurotoxicity induces cleavage of p35 to p25 by calpain. *Nature* 405(6784):360–364.
57. Giusti-Rodríguez P, et al. (2011) Synaptic deficits are rescued in the p25/Cdk5 model of neurodegeneration by the reduction of β-secretase (BACE1). *J Neurosci* 31(44): 15751–15756.
58. Fukumoto S, et al. (2001) Akt participation in the Wnt signaling pathway through Dishevelled. *J Biol Chem* 276(20):17479–17483.
59. Zhang J, Li H, Herrup K (2010) Cdk5 nuclear localization is p27-dependent in nerve cells: Implications for cell cycle suppression and caspase-3 activation. *J Biol Chem* 285(18):14052–14061.
60. Fang WQ, Chen WW, Fu AK, Ip NY (2013) Axin directs the amplification and differentiation of intermediate progenitors in the developing cerebral cortex. *Neuron* 79(4):665–679.
61. Comeau SR, Gatchell DW, Vajda S, Camacho CJ (2004) ClusPro: An automated docking and discrimination method for the prediction of protein complexes. *Bioinformatics* 20(1):45–50.